

Infrared absorption due to local vibrational modes of nitrogen in GaAs:N and GaAs-based dilute nitrides

This article has been downloaded from IOPscience. Please scroll down to see the full text article.

2004 J. Phys.: Condens. Matter 16 S3037

(<http://iopscience.iop.org/0953-8984/16/31/004>)

View [the table of contents for this issue](#), or go to the [journal homepage](#) for more

Download details:

IP Address: 129.252.86.83

The article was downloaded on 27/05/2010 at 16:21

Please note that [terms and conditions apply](#).

Infrared absorption due to local vibrational modes of nitrogen in GaAs:N and GaAs-based dilute nitrides

Hans Christian Alt

Engineering Physics Department, FHM—Munich University of Applied Sciences,
Postfach 20 01 13, D-80001 München, Germany

Received 5 February 2004

Published 23 July 2004

Online at stacks.iop.org/JPhysCM/16/S3037

doi:10.1088/0953-8984/16/31/004

Abstract

This paper reviews recent experimental progress in the investigation of nitrogen in GaAs and GaAs-based dilute nitrides by Fourier transform infrared absorption spectroscopy. Isolated substitutional nitrogen on the anion site gives rise to a local vibrational mode at a wavenumber of 472 cm^{-1} , which can be detected at low temperatures as a sharp absorption band. Based on a comparison with secondary ion mass spectroscopy and x-ray diffraction analysis, a calibration factor is derived for the integrated absorption of the band. Quantitative determination of substitutional nitrogen is possible in epitaxial layers of only 10 nm thickness. The influence of indium–nitrogen bonding on the local mode frequency is discussed. A mode at 490 cm^{-1} is tentatively attributed to the InGa_3N configuration. An additional local vibrational mode occurs at 638 cm^{-1} . A valence-force model is presented, which reproduces quantitatively the experimentally observed host-isotope fine structure. The results are consistent with an assignment to a nitrogen–gallium vacancy complex.

1. Introduction

Local vibrational mode (LVM) spectroscopy is particularly suitable for the investigation of light impurities in gallium arsenide lattice, because LVMs can often be detected as sharp bands in low-temperature infrared (IR) absorption spectra, energetically well above the strong LO phonon band at around 300 cm^{-1} . From LVM spectroscopy it is known, for example, that boron, carbon and silicon usually form simple substitutional defects, with B_{Ga} , C_{As} and Si_{Ga} , respectively, being the most common species [1–4]. Hydrogen, like in other semiconductors, is mainly incorporated in complexes, preferably in hydrogen-acceptor and hydrogen-donor centres [5]. Oxygen occurs interstitially, however also in an off-centre position, close to the As lattice site [6, 7].

Until recently, the knowledge about LVMs due to nitrogen in GaAs was comparatively scarce. Optically detected evidence for nitrogen in GaAs was first reported by Kachare *et al* [8]. After implantation of high-energy $^{14}\text{N}^+$ ions into semi-insulating (SI) GaAs, a broad band at 480 cm^{-1} was observed in IR absorption. The band was attributed to substitutional nitrogen, N_{As} . Further work was done on epitaxially grown GaAs:N. Using vapour phase epitaxy with NH_3 added to the carrier gas, nitrogen-doped epitaxial layers of GaAs were grown [9, 10]. These layers also show nitrogen-related absorption at about 470 cm^{-1} . In bulk crystals, N–H complexes have also been found, identified by the high-frequency hydrogen vibrations between 1000 and 3000 cm^{-1} [11].

New interest in LVM spectroscopy of nitrogen in GaAs-based materials arose with the advance of GaAsN and InGaAsN layers, grown by molecular beam epitaxy (MBE) or metal organic chemical vapour deposition (MOCVD) [12, 13]. The epitaxial layer quality is strongly dependent on the incorporation behaviour of nitrogen. Therefore, it is highly desirable to have experimental techniques available for characterization of the various nitrogen species, which may occur in the material, such as substitutional, interstitial or clustered nitrogen. Photoluminescence (PL) can be used to determine the band gap and the optical emission efficiency. Annealing usually leads to a large increase of the PL intensity and a blue shift of the peak emission wavelength. Both effects are attributed to a redistribution of nitrogen during annealing [14, 15]. The substitutional nitrogen fraction x itself is usually derived from x-ray diffraction (XRD) analysis, assuming Vegard's law to be valid for the lattice constant.

Both PL and XRD are only indirect methods to assess the incorporation of nitrogen in the layer. Secondary ion mass spectroscopy (SIMS) is possible, due to the high nitrogen concentration. The drawback is that it measures the total chemical nitrogen concentration. Other techniques, such as high-resolution microscopy, are not suitable for routine application. On the other hand, typical defect concentrations for LVM spectroscopy are in the range of parts per million (ppm), or even below. State-of-the art (In)GaAsN layers, however, contain nitrogen up to 6% ($x = 0.06$), corresponding to nitrogen concentrations of the order of 10^{20} or even 10^{21} cm^{-3} . It was not clear *a priori*, whether LVM spectroscopy could provide useful information on the incorporation behaviour of nitrogen in this alloy regime. It is therefore the aim of this paper to familiarize the reader with the recent developments and to demonstrate the power of LVM absorption spectroscopy in this field, covering nitrogen defect concentrations from 10^{14} up to 10^{21} cm^{-3} .

2. Experimental details

Nitrogen-rich bulk GaAs samples were selected from commercial material with respect to the nitrogen concentration, as measured by radio frequency spark source mass spectrometry (SSMS) under ultrahigh vacuum conditions. The equipment is an upgraded high-resolution 21-110 type Mattauch-Herzog mass spectrometer with simultaneously detecting ion sensitive Q plate and a computerized Syncotec microdensitometer.

GaAsN films were deposited on (001)-oriented semi-insulating GaAs substrates in a vertical high-speed rotating-disc MOCVD reactor at temperatures between 500 and $650\text{ }^\circ\text{C}$. Triethylgallium (TEG), tertiary butyl arsine (TBA) and unsymmetric dimethylhydrazine (DMH) were used as precursor compounds. The nitrogen-containing film had a thickness of about 60 nm and was capped by pure GaAs of 12 nm thickness. As-grown and annealed samples were available. Annealing was performed at $700\text{ }^\circ\text{C}$ in the reactor. The nitrogen content was determined by XRD and SIMS. Rocking curves were recorded around the symmetric (004) reflection and the asymmetric (115) reflection. The measurements showed that the layers are fully pseudomorphic. SIMS measurements were performed to determine the

total chemical nitrogen content. Cs⁺ ions with energy of 5.5 keV were used as primary ions. The measurements were calibrated with the help of nitrogen-implanted GaAs substrates. The total chemical nitrogen content, for the samples investigated by LVM absorption, was between 0.005 and 0.054, with higher values for lower growth temperature.

Further GaAsN and InGaAsN layers were grown by solid-source MBE on semi-insulating GaAs(001) substrates. A radio-frequency-coupled plasma source was used to generate the reactive nitrogen species from N₂. Ternary alloys were grown up to 3 μm thick. Quaternary alloys were produced as multiple-quantum-well (MQW) structures with up to 5 quantum wells of up to 10 nm thickness. The nitrogen content x was between 0.003 and 0.027 (according to XRD), and the indium content y between 0.3 and 0.4. Standard annealing was performed *in situ* at 750 °C; for comparative purposes some of the samples were annealed *ex situ* under similar conditions.

Nitrogen-implanted samples were prepared from commercial carbon-doped semi-insulating GaAs wafers with (100) orientation grown by the liquid encapsulated Czochralski (LEC) or vertical gradient freeze (VGF) technique. Implantation of the nitrogen isotope ¹⁴N was carried out with a set of different ion energies up to 400 keV to obtain a nearly uniform nitrogen concentration of about $2.2 \times 10^{20} \text{ cm}^{-3}$ (corresponding to 1% of the anion lattice sites) in the depth between 0.2 and 0.7 μm. The total dose was $1.75 \times 10^{16} \text{ cm}^{-2}$. During implantation, the samples were tilted by 7° with respect to the ion beam, to avoid channelling. The sample holder was either kept at room temperature (RT) or cooled by liquid nitrogen. Another series of samples was generated by high-energy (3 MeV) implantations of ¹⁴N and/or ¹⁵N. In this case, the total dose was $1 \times 10^{16} \text{ cm}^{-2}$ and the sample temperature was close to RT.

Rapid thermal annealing (RTA) was done in the temperature range between 450 and 900 °C under flowing nitrogen gas, with the implanted sample surface covered by another virgin GaAs wafer (face-to-face technique). In some samples, the nitrogen profiles before and after annealing were checked by SIMS.

Fourier transform infrared (FTIR) absorption measurements were performed in the wavenumber range from 200 to 3000 cm⁻¹, using a high-resolution vacuum instrument (Bruker IFS 113v). A globar source, a Mylar beam splitter and triglycine sulfate or mercury cadmium telluride detectors were used for the far-infrared and mid-infrared region, respectively. A continuous-flow cryostat with caesium iodide optical windows allowed the sample temperature to be kept in the range between 10 and 300 K.

Although the nitrogen-related bands are detectable also at room temperature, the samples were held at a temperature of about 77 K or at 10 K, as the background absorption of the GaAs matrix is reduced and the bands are sharper. Standard spectra were recorded using a resolution of 2.5 cm⁻¹ in order to suppress interference fringes coming from the substrate. High-resolution spectra (up to a resolution of 0.03 cm⁻¹) were taken from samples with wedged surfaces.

3. The localized vibrational mode of substitutional nitrogen in nitrogen-rich bulk GaAs crystals

Nitrogen is present during crystal growth of GaAs as N₂ gas, used as an ambient gas in the liquid encapsulated Czochralski (LEC) or vertical gradient freeze (VGF) process, or as a constituent of the pyrolytic boron nitride (pBN) used for the crucible. From radio-frequency spark source mass spectrometry (SSMS) [16], it is known that commercial semi-insulating (SI) LEC GaAs grown under nitrogen atmosphere contains nitrogen in the 10^{15} cm^{-3} range. In the polycrystalline starting material the concentration can be even higher, by an order of magnitude.

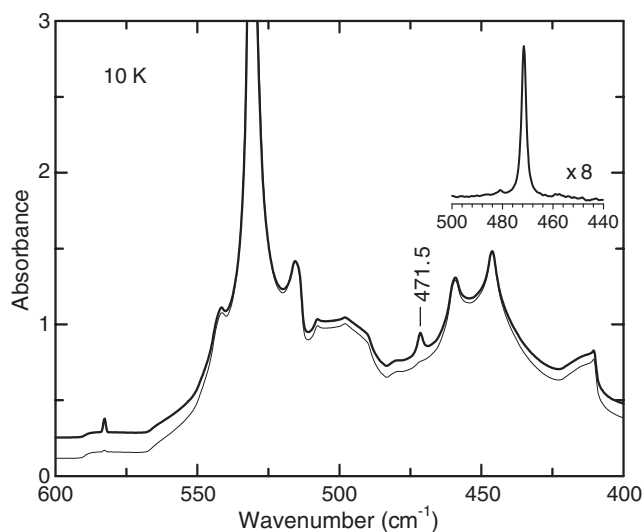


Figure 1. Low-temperature FTIR absorption spectra of nitrogen-rich (bold curve) and nitrogen-lean (small curve) GaAs. The inset shows the N-related LVM obtained from the difference spectrum.

GaAs samples with a chemical N concentration above 10^{15} cm^{-3} (as determined by SSMS) always show a band at about 472 cm^{-1} in the infrared absorption spectrum (figure 1). The line is superimposed to the multiphonon spectrum of GaAs, between the TO + LA structure at $\sim 450 \text{ cm}^{-1}$ and the strong 2 TO structure at $\sim 525 \text{ cm}^{-1}$ [17]. For the quantitative evaluation of the line, the absorption spectrum of a nitrogen-lean (below the SSMS detection limit of $1 \times 10^{14} \text{ cm}^{-3}$) LEC GaAs sample was subtracted.

From its first observation in N-implanted samples, it has been suggested that the 472 cm^{-1} line is due to N_{As} [8]. This assignment is mainly driven by the plausible argument that a group V impurity will substitute the anion in a III-V semiconductor and by the similarity to N in GaP. Nitrogen doping in GaP has been studied extensively because of the importance for the light-emitting process in GaP-based diodes [18].

The assignment has now become clear due to implantation experiments with ^{14}N and ^{15}N in bulk GaAs [19] (see figure 2). After RTA at 600°C , ^{14}N -implanted samples show a band with a maximum at $472.0 \pm 0.5 \text{ cm}^{-1}$ (at 77 K). Implantation of the isotope ^{15}N causes a shift of this band towards lower frequencies with a new maximum at $457.0 \pm 0.5 \text{ cm}^{-1}$. The question whether one or more N atoms are involved has been resolved by mixed isotope implantations. The result of the sample implanted with equal doses of ^{14}N and ^{15}N (figure 2) is unambiguous: two clearly resolved bands are observed. The peak positions coincide with the peak position found after implantation of either the ^{14}N or the ^{15}N isotope. This is exactly what is expected for a nitrogen defect containing one impurity atom.

Assuming a simple defect model with one vibrating nitrogen atom in an otherwise rigid lattice, the replacement of ^{14}N by ^{15}N should lead to an LVM frequency ratio $\omega(^{14}\text{N})/\omega(^{15}\text{N})$ equal to $[m(^{15}\text{N})/m(^{14}\text{N})]^{1/2} = 1.035$. The observed ratio is 1.033 ± 0.002 ; therefore, the agreement is excellent. In the case of the thoroughly studied anion sites impurities $^{12}\text{C}_{\text{As}}/^{13}\text{C}_{\text{As}}$ and $^{10}\text{B}_{\text{As}}/^{11}\text{B}_{\text{As}}$, the experimentally observed isotope shift amounts to 92% and 91%, respectively, of the theoretically expected value [20, 21]. A lower isotope shift occurs if vibrational motion of the neighbouring host atoms is included in the model. Therefore, it must be concluded that the 472 cm^{-1} LVM is strongly localized at the defect site.

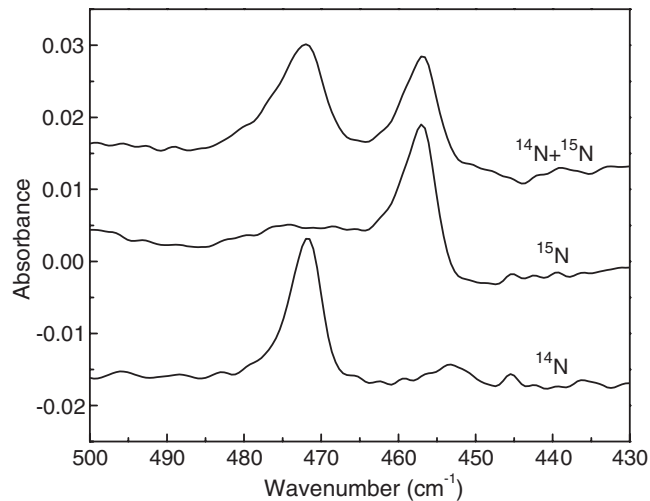


Figure 2. Spectra of ^{14}N and ^{15}N -implanted samples after subtraction of the reference. Spectra are shifted vertically for clarity.

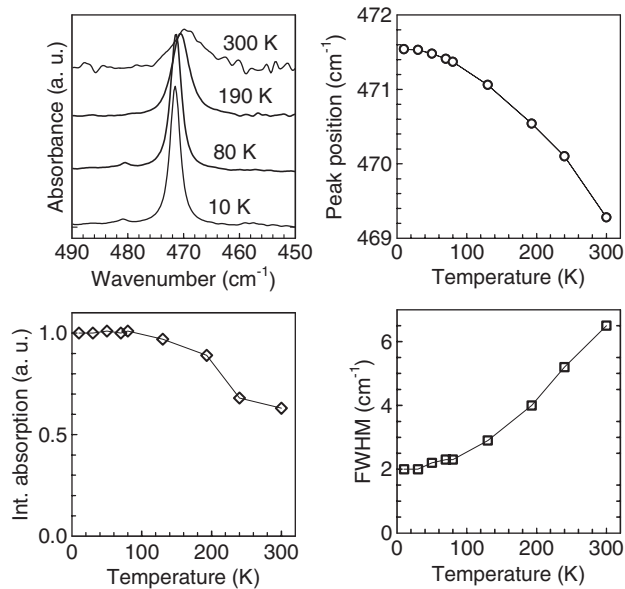


Figure 3. Line shape and line shape parameters of the 472 cm^{-1} band due to N_{As} as a function of temperature.

The nearest-neighbour atoms of the N_{As} defect are gallium atoms. Therefore, fine-structure splitting of the band due to the host isotopes ^{69}Ga and ^{71}Ga should be expected. However, this is not the case. The band is comparatively broad ($\text{FWHM} \approx 2.0\text{ cm}^{-1}$) and has no structure [22]. Line broadening can be caused by a reduced lifetime of the vibrational state. In the case of the 472 cm^{-1} vibration, it can be assumed that elastic scattering of band phonons is the dominant process [23]. Unfortunately, no quantitative theory is at present available. The question whether lifetime can explain the width of the 472 cm^{-1} band has to be answered by future theoretical work.

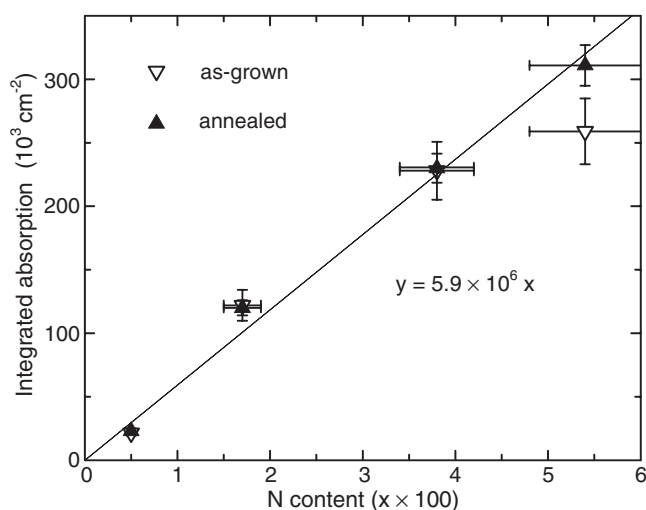


Figure 4. Integrated absorption of the N_{As} LVM absorption band as a function of the nitrogen content x (MOCVD-grown samples). The straight line is a fit through the origin.

Details of the temperature dependence are shown in figure 3. The peak position of the band shifts from 471.54 cm^{-1} at 10 K to 469.39 cm^{-1} at 300 K. The FWHM increases from 2.0 to 6.4 cm^{-1} . It should also be mentioned that a very small side band exists at 480.9 cm^{-1} . No identification has been found so far for this band. It can be detected up to temperatures of 100 K. At higher temperatures it merges with the main band. No thermal activation was detected in this limited temperature range [22].

4. The situation in epitaxially grown GaAsN: quantitative aspects

Substitutional nitrogen can be detected by LVM spectroscopy also in thin epitaxial layers of GaAsN and InGaAsN, grown by MBE or MOCVD. In the case of technologically important nitrogen concentrations of $>1\%$, a layer thickness of about 10 nm of high-quality epitaxial material is sufficient for the detection of the 472 cm^{-1} band. Nevertheless, it is of crucial importance, whether LVM spectroscopy is able to provide quantitative results. If it is, then FTIR LVM spectroscopy is the method of choice for the assessment of the substitutional nitrogen concentration in such layers.

From theory [24], the integrated absorption (IA) of the LVM absorption band is related to the number of oscillators D (per cm^3) by (in SI units)

$$IA = q^2 / (4\epsilon_0 n c^2 \mu) D, \quad (1)$$

where q is the effective charge of the induced electric dipole, μ the reduced mass of the vibrating entity, n the refractive index of the material, ϵ_0 the permittivity constant, and c the velocity of light.

The result of the analysis in a series of well-characterized samples grown by MOCVD is shown in figure 4. XRD and calibrated SIMS measurements give the same nitrogen content in these layers within experimental error [25]. These data are plotted on the abscissa. No significant change of the IA of the N_{As} LVM is found before and after annealing (700°C , *in situ*), except for the epitaxial layer with the highest nitrogen content ($x = 0.054$). The increase of the IR signal is slightly beyond experimental error ($\pm 10\%$). No change is found

by SIMS measurements before and after annealing. Therefore, the total chemical nitrogen content remains unaffected by annealing. One explanation would be that the increase of the IA is caused by a reduction of interstitial and a corresponding increase of substitutional nitrogen, as is discussed in the context of annealing [26].

After annealing, a good linear relationship exists between the IA and the nitrogen content, as determined by XRD and SIMS. We conclude that, after annealing, within experimental error of about 10%, only substitutional nitrogen is present in the alloy. A calibration of the LVM absorption band in terms of the IA, defined by

$$IA = Cx \quad (2)$$

gives $C = 5.9 \times 10^6 \text{ cm}^{-2}$ (see the fitted line in figure 4). We also investigated a considerable number of samples grown by MBE, with $x \leq 0.02$, characterized by XRD only in the centre of the wafer. The correlation between the IA of the N_{As} LVM and the nitrogen content x gives a value for C which is not significantly different from the result based on MOCVD-grown samples only [27]. It is therefore concluded that the measurement of the LVM absorption by FTIR allows a rapid and reliable determination of the substitutional nitrogen content in both MOCVD- and MBE-grown epitaxial layers in the range $0 < x < 0.06$.

For a comparison with well-established LVM calibrations for other light impurity defects, occupying lattice sites in GaAs, it is more convenient to use the expression derived from equation (1):

$$D = f \times IA. \quad (3)$$

The constant f is usually referred to as the calibration factor. Using the density of atoms in the GaAs crystal of $4.4 \times 10^{22} \text{ cm}^{-3}$, the calculation of f_N for the N_{As} LVM gives $f_N = 3.7 \times 10^{15} \text{ cm}^{-1}$.

This value is roughly by a factor of 2 smaller than the corresponding value for C_{As} , and more than an order of magnitude smaller than for the other defects [27]. From equation (1) it can be inferred that this must be due to a large effective charge q . This parameter essentially includes the induced electric dipole moment [24]. Two peculiarities of the nitrogen defect must be kept in mind. First, N_{As} is an isoelectronic centre, whereas the other impurities, aside from B_{Ga} , act as donors or acceptors. These latter defects are usually investigated in their charged state. However, as far as experimental information is available, the effect of the missing or additional valence electron on the strength of the LVM absorption band is small. Second, nitrogen is a small atom compared to the substituted arsenic atom, and is strongly electronegative. Therefore, the Ga–N bond has a high polarity. We suggest that the polarity of the bond leads to the relatively large induced electric dipole moment. An increase of roughly 50% in comparison with C_{As} is necessary to comply with the experimental data. This seems reasonable in view of the smaller electronegativity of carbon compared to nitrogen.

The data presented cover defect concentrations in the range of 10^{20} – 10^{21} cm^{-3} . To our knowledge, there is at present no other calibration for LVM absorption in GaAs in this high concentration range. The strict proportionality of the IA to the defect concentration according to equation (1) is valid only for isolated, non-interacting centres. Furthermore, the defect density must be low enough to represent a weak perturbation for the phonon density of states of the (GaAs) matrix crystal. Both assumptions may be questioned for nitrogen in epitaxially grown GaAsN layers, since, for example, a nitrogen fraction x of 0.03 means that, statistically, in one direction roughly every sixth atom is an N atom.

Model calculations, performed for B_{As} and C_{As} [28], point out that the vibrational amplitude of an LVM essentially vanishes beyond the second nearest-neighbour of the defect. The previous experimental study on the $^{14}N_{As}/^{15}N_{As}$ isotope shift also indicates a strong spatial localization for the LVM of N_{As} . Nevertheless, some vibrational coupling between

neighbouring nitrogen atoms cannot be ruled out at such high concentrations. There is also experimental evidence from scanning tunnelling microscopy that a modest pairing of nitrogen atoms occurs on second nearest-neighbour sites [29]. Further studies are certainly necessary to evaluate the influence of these effects on the LVM of N_{As} in the concentration range investigated. It should be emphasized that such complications do not affect the validity of the calibration given above, at least within the experimental accuracy of about 10%. At present, we have no experimental evidence for a significant deviation from a linear correlation between the IA of the LVM and the substitutional nitrogen defect concentration. It is also possible to detect the 472 cm^{-1} LVM in GaAsN layers by Raman spectroscopy [30]. Consistent with our findings, Mascarenhas and Seong [31] reported that the normalized Raman intensity exhibits a linear dependence on the nitrogen concentration for $x \leq 0.03$.

5. The local environment of nitrogen in InGaAsN layers

The optical and electronic properties of the quaternary system $\text{In}_y\text{Ga}_{1-y}\text{As}_{1-x}\text{N}_x$ depend on the microscopic spatial arrangement of the alloy elements. The simplest case is a statistical distribution of indium and gallium on the cation sites and arsenic and nitrogen on the anion sites, respectively. This is called a random alloy. Another possibility is some kind of ordering. For example, nitrogen could preferably form bonds with indium, and arsenic with gallium. In that sense, one could think of the quaternary alloy of being composed of two binaries, InN and GaAs.

Recent theoretical investigations using Monte Carlo simulations strongly favour an increase of In–N and Ga–As bonds relative to the random situation [32]. The argument is that the local coordination of the large indium atom with the small nitrogen atom significantly reduces the strain energy in the alloy, overcompensating the loss of cohesive energy caused by the lower bond strength of In–N compared to Ga–N.

LVM spectroscopy should be particularly sensitive to changes of the local environment of substitutional nitrogen in quaternary InGaAsN. The replacement of gallium atoms on nearest-neighbour sites by indium atoms has an impact on the LVM frequency as, due to the different bond strength, the force constant of the In–N bond is different from that of the Ga–N bond. The size of the effect can be estimated from the LVM frequency of substitutional nitrogen in bulk InAs, which can be considered as the limiting case of $\text{In}_y\text{Ga}_{1-y}\text{As}_{1-x}\text{N}_x$ with $y = 1$. Again using ion implantation of ^{14}N and ^{15}N into bulk InAs material, we found LVM frequencies of 443 and 429 cm^{-1} , respectively [33]. The frequency downshift relative to GaAs must be expected, as the LO phonon frequency is 254 cm^{-1} in InAs compared to 296 cm^{-1} in GaAs.

For $\text{In}_y\text{Ga}_{1-y}\text{As}_{1-x}\text{N}_x$ with $0 < y < 1$, five different local arrangements ('molecules') are possible: Ga_4N , InGa_3N , $\text{In}_2\text{Ga}_2\text{N}$, In_3GaN and In_4N . Due to symmetry lowering from tetrahedral symmetry (T_d), actually nine different modes are expected for N_{As} in InGaAsN alloys. The very similar case of C_{As} in AlGaAs alloys has been investigated theoretically by Sangster *et al* [34] using cluster calculations. The general trend is that the LVM frequencies of the mixed configurations are distributed between the frequencies of the pure configurations. However, notable exceptions exist if new equilibrium positions of the constituents of the defect molecule are associated with changes of the force constants. This has to be taken into account if the large indium atom replaces a gallium atom.

We studied $\text{In}_y\text{Ga}_{1-y}\text{As}_{1-x}\text{N}_x$ layers, grown by MBE, with an indium fraction y between 0.3 and 0.4 and a nitrogen fraction x up to 0.02. A typical low-temperature (77 K) FTIR absorption difference spectrum of an MQW structure ($x = 0.018$, $y = 0.35$), with five quantum wells of a thickness of 10 nm each, is shown in figure 5. A sharp band is found at 471.4 cm^{-1} . The band position is identical to the LVM of substitutional nitrogen in pure

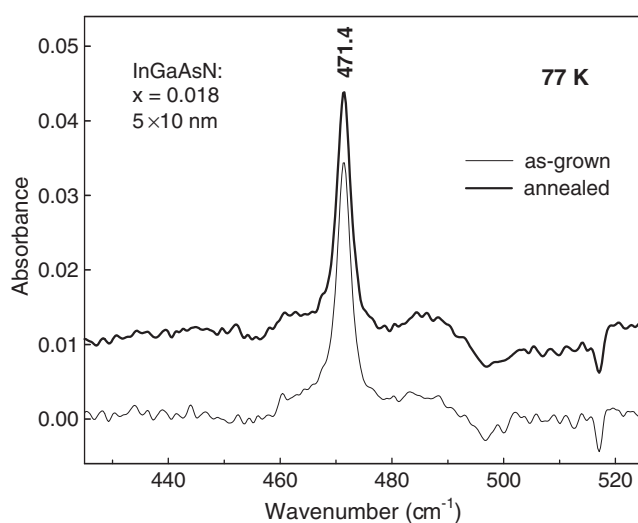


Figure 5. Low-temperature FTIR absorption spectra of a $\text{In}_y\text{Ga}_{1-y}\text{As}_{1-x}\text{N}_x$ MQW structure with $y = 0.35$ and $x = 0.018$ before and after (*ex situ*) annealing at 750°C . The reference spectrum has been subtracted. The spectrum of the annealed sample has been displaced vertically for clarity.

GaAs. The FWHM of about 3.0 cm^{-1} is smaller than in the ternary alloy GaAsN and not much larger than in bulk crystals (2.0 cm^{-1}). This is indicative of the high quality of the MBE layer. No change of the LVM signal can be detected after annealing at 750°C , either in the strength or in the position of the band. The effect of annealing is, as usually observed, a large increase of the PL intensity. Evidently, this enhancement is not related to a substantial change of the substitutional nitrogen concentration itself, but probably to annealing of nonradiative recombination centres.

In a random alloy with $y = 0.35$, the probability that 0, 1, 2, 3, and 4 nearest-neighbour indium atoms surround a nitrogen atom on the anion site, is 0.179, 0.384, 0.311, 0.111, and 0.015, respectively. Therefore, molecular configurations with 1 or 2 indium atoms are most probable. The fact that only the pure GaAs-like configuration is observed leads—for the MBE-grown InGaAsN MQW structures investigated—to the unambiguous conclusion that nitrogen bonds only with gallium atoms.

The results obtained by other groups provide no clear picture. FTIR measurements on thick epitaxial layers grown by MOCVD with 2.5% indium and 0.2% nitrogen reveal additional LVM bands at 457 and 487 cm^{-1} after annealing [35]. The new bands are attributed to the formation of In–N bonds and the associated strengthening of Ga–N bonds. A band at 489 cm^{-1} is also observed by FTIR in material containing 5% indium and 2% nitrogen, which was grown by gas-source MBE [36]. This is probably the same feature as the 487 cm^{-1} LVM, since it increases with annealing temperature. Raman measurements on MBE-grown layers with 12% indium and 4% nitrogen show three peaks at 425 , 458 , and 480 cm^{-1} [37]. The frequency shifts relative to the 470 cm^{-1} Raman signal in pure GaAsN are also attributed to changes of the bond state of nitrogen due to the incorporation of indium.

The existence of an LVM frequency at around 490 cm^{-1} in InGaAsN is confirmed by our own investigations of GaAs samples, which were co-implanted with indium and nitrogen. After RTA at 800°C , this band appears, correlated with the ratio of indium to nitrogen in the implanted layer (figure 6). We suggest that it corresponds to the nitrogen configuration with one indium atom on a nearest-neighbour site, which would then be the manifestation of the

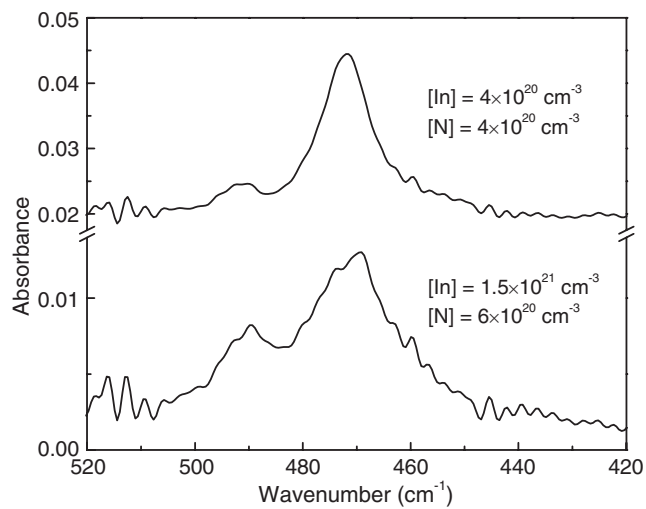


Figure 6. FTIR spectra for GaAs layers implanted with indium and nitrogen.

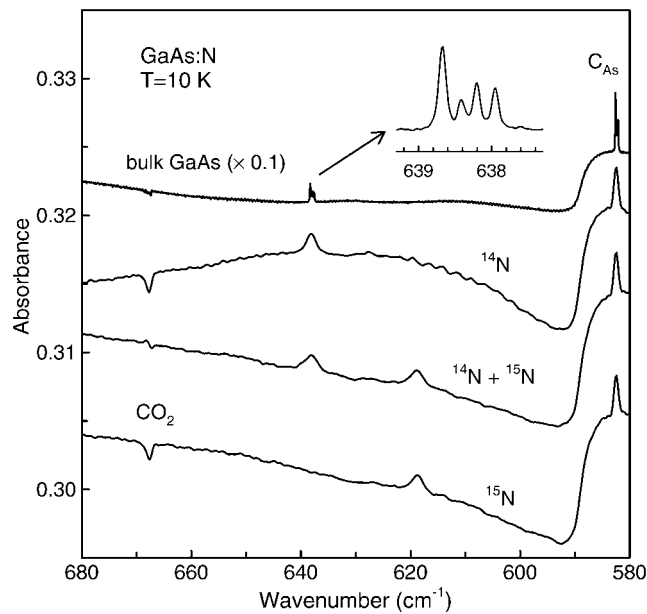


Figure 7. Mid-infrared spectra of samples implanted with 3 MeV nitrogen isotopes ^{14}N and ^{15}N after RTA at 600°C . The spectrum of a nitrogen-rich bulk GaAs sample is also shown. The fine structure of the LVM at 638 cm^{-1} in this sample is given in the inset.

InGa_3N molecule. The shift to higher frequency should, indeed, be due to the shortening of the Ga–N bond length, caused by the larger indium atom.

X-ray absorption fine structure spectroscopy (XAFS) is also sensitive to the chemical environment of nitrogen. In MBE-grown InGaAsN with 30% indium and 3% nitrogen, a random distribution is found in the as-grown state, whereas the annealed material exhibits a pronounced In–N coordination [38]. On the other hand, using the same technique, only

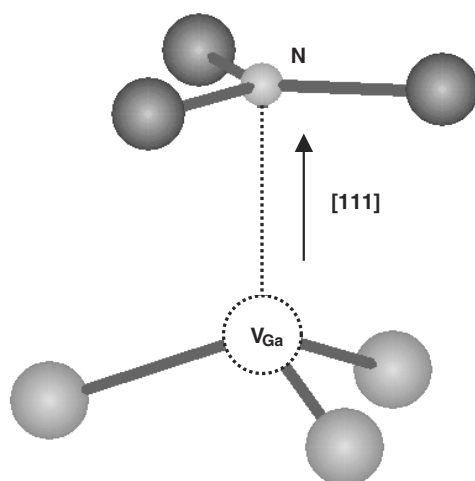


Figure 8. A structural model of the N- V_{Ga} complex.

a small In-N ordering effect is found after RTA at 700 °C, in layers containing 4% indium and 2–3% nitrogen [39]. The interpretation of XAFS spectra seems to be difficult and needs careful model simulations, in particular, because the influence of preferred In-N bonding on the spectra is only moderate.

Taking all this together, it is obvious that at present the understanding, experimental and theoretical, of the local structure around the nitrogen atom in InGaAsN is far from being complete. Several parameters have to be taken into account: the growth technique, the indium and the nitrogen content, the annealing state, etc. A crucial question certainly is how close (how far) the system is to (from) thermodynamic equilibrium.

6. The nitrogen-gallium vacancy defect

An LVM band at 638 cm^{-1} with a characteristic fine-structure pattern of four resolved components is occasionally observed in bulk GaAs crystals. Recently, this band was tentatively related with nitrogen [40], based on the appearance in crystals grown by the LEC technique under N_2 overpressure. We found that this band can be generated reproducibly in GaAs samples after nitrogen implantation and RTA in the temperature range between 600 and 800 °C.

Usually, after implantation of the ^{14}N isotope, a weak 638 cm^{-1} band can be detected (see figure 7). The band shifts to 619 cm^{-1} if the heavier isotope ^{15}N is implanted. This is an unambiguous proof that the band is caused by an LVM due to the implanted nitrogen. The relative shift amounts to 3.0% whereas, from the inverse proportionality to the square root of the isotope mass, a shift of 3.4% would be expected. In the case of co-implantation of ^{14}N and ^{15}N , both bands are found, but no further band. Therefore, it is again clear that only one nitrogen atom is involved in this centre.

The fine structure of the 638 cm^{-1} band in bulk crystals is also shown in figure 7. The splitting between the individual lines is about 0.2 cm^{-1} , and the FWHM of the lines is $0.10 \pm 0.01\text{ cm}^{-1}$. The pattern is definitely different from that observed in the case of simple substitutional defects on the anion lattice site, such as C_{As} or Si_{As} [41]. In implanted samples, the band does not show the fully resolved fine structure. We believe that this is due to line broadening caused by residual strain within the implanted layers. All that has been

Table 1. Calculated frequencies (in cm^{-1}) and statistical probabilities for all modes of the $^{14}\text{N}\text{Ga}_3$ molecule in GaAs. The experimental frequencies, presented for comparison, have an uncertainty of $\pm 0.01 \text{ cm}^{-1}$.

Configuration	Mode	Probability	Calculated frequency	Experimental frequency
$^{14}\text{N } ^{71}\text{Ga}_3$	E	0.0635	637.95	637.95
$^{14}\text{N } ^{71}\text{Ga}_2 \text{ } ^{69}\text{Ga}_1$	A'	0.1435	638.43	638.41
	A''	0.1435	637.95	
$^{14}\text{N } ^{71}\text{Ga}_1 \text{ } ^{69}\text{Ga}_2$	A'	0.2162	638.19	638.20
	A''	0.2162	638.67	
$^{14}\text{N } ^{69}\text{Ga}_3$	E	0.2171	638.67	638.67

found so far is an asymmetry of the band with an indication of a peak at the position where the strongest of the four lines of the fine structure should appear [42].

An identical four-line pattern has been reported from a band at 577 cm^{-1} in carbon-doped GaAs after irradiation with 2 MeV electrons or fast neutrons [43, 44]. Neglecting the small perturbation caused by the different host isotopes, the well-known substitutional carbon defect, $^{12}\text{C}_{\text{As}}$, has T_d symmetry and a threefold degenerate LVM with a frequency of 583 cm^{-1} (10 K). Lowering the defect symmetry to C_{3v} leads to a splitting into a longitudinal A_1 mode and a transverse E mode. The E mode is responsible for the absorption at 577 cm^{-1} . By adjusting the force constants within the framework of a Keating model, it is possible to reproduce the fine structure.

For a corresponding analysis of the 638 cm^{-1} band, we used a simple valence force model, taking into account only central forces between the nitrogen atom and its neighbouring gallium atoms [45]. The model includes a possible relaxation of the nitrogen atom from the tetrahedral position in a [111] direction. Due to the inherent C_{3v} symmetry of the model, three of the four neighbouring gallium atoms are equivalent. If the various configurations of the two Ga isotopes are considered, the fine structure of the band found experimentally is qualitatively reproduced; however, the splitting between the lines is too large. This effect is well known, and is due to the neglected interaction between the neighbouring gallium atoms and the surrounding host atoms [24]. It has been shown [46] that a correction is possible in first order by multiplying the gallium mass with a constant factor $\chi > 1$.

Further analysis was performed using the mass factor χ as a parameter to fit the splitting between the outermost lines. The bond stretching force constant between the nitrogen atom and the three equivalent gallium atoms was then adjusted to obtain the required frequency. As the vibrational amplitude of the E mode is orthogonal to the bond in the direction with the remaining gallium atom, this force constant has no influence. The quality of the fit is independent of a possible relaxation of the nitrogen atom. As expected, the outermost lines are due to the twofold degenerate E mode of the isotopically pure configurations $^{14}\text{N } ^{71}\text{Ga}_3$ and $^{14}\text{N } ^{69}\text{Ga}_3$, respectively, with true C_{3v} symmetry. The mixed configurations $^{14}\text{N } ^{71}\text{Ga}_2 \text{ } ^{69}\text{Ga}_1$ and $^{14}\text{N } ^{71}\text{Ga}_1 \text{ } ^{69}\text{Ga}_2$ have C_s symmetry, due to the perturbation by the different gallium isotopes. The A'' modes of these configurations have the same frequency as the E modes of the pure configurations, whereas the A' modes are responsible for the inner lines (see table 1).

The intensity of the lines can be calculated if it is assumed that the gallium isotopes ^{69}Ga (60.1% abundance) and ^{71}Ga (39.9% abundance) are randomly distributed. The degeneracy of the modes (2 for an E mode, 1 for an A' or A'' mode) and the number of geometrical arrangements leading to the same configuration have to be taken into account. The result is also given in table 1.

From the good agreement with experiment, concerning line splittings and intensity ratios, we conclude that the vibrational state is correctly reproduced by the model. Certainly, the reason for the symmetry lowering from T_d to C_{3v} needs discussion. In all samples, the majority of the incorporated nitrogen atoms occupy substitutional (T_d) sites¹. Consequently, a perturbation of the local nitrogen environment is needed to induce the required symmetry lowering. Based on an estimate of the defect concentration involved in the 638 cm^{-1} band in nitrogen-implanted samples, it can be shown that the participation of another chemical impurity can be excluded [42]. This means that either nitrogen itself, by forming a complex, or an intrinsic defect, such as an interstitial or a vacancy, must be the origin. We argue that the experimental data and model calculations favour a nitrogen–gallium vacancy pair.

From the model calculations it is found that the increase of the N–Ga force constant in the case of the 638 cm^{-1} LVM amounts to 60–80% in comparison with the 472 cm^{-1} mode, dependent on the amount of relaxation in the [111] direction. The only reasonable explanation for such behaviour is a considerable bond shortening between nitrogen and gallium. This is supported by the fact that, for isolated substitutional nitrogen in GaAs, the N–Ga bond is indeed under tensile strain. The anion–cation bond length in pure GaAs is 0.245 nm compared to 0.195 nm in pure GaN, amounting to a difference of about 25%. Assuming no relaxation of the surrounding Ga atoms, the maximum displacement of the N atom from the tetrahedral position to an in-plane configuration with three nearest-neighbour Ga atoms would reduce the N–Ga bond length by 6%, implying that the bond is still elongated. On the other hand, theoretical calculations based on a large supercell approach [47] predict that the N–Ga bond length for N_{As} in GaAs is only 5–6% larger than in pure GaN, due to an inward relaxation of the Ga atoms. Keeping the positions of the Ga atoms fixed, the in-plane configuration of the nitrogen atom would then bring the N–Ga bond length close to its value in GaN.

From our model, it is not possible to obtain any information on the bonding of the nitrogen atom in the direction opposite to the relaxation. However, the most natural explanation is that there is no bond at all, due to the presence of a gallium vacancy. The lacking bond can then be considered as the catalyst for the relaxation. The relatively high defect concentration found in implanted samples is in agreement with this assumption, as a large number of vacancies are expected from irradiation damage. On the contrary, it is not clear how interstitials could be involved. Even disregarding the problem of finding a proper defect model, it is unlikely that interstitials will survive the high-temperature RTA treatment. Concerning nitrogen itself, it is certainly possible that some sort of nitrogen pairing or clustering could occur with nitrogen atoms on more distant shells; however, this would not explain the large increase of the N–Ga bond strength in the core of the defect.

We conclude that

- (i) the relaxation of the threefold coordinated nitrogen in the 638 cm^{-1} centre is large enough to place the nitrogen atom close to an in-plane configuration with its three nearest-neighbour gallium atoms, and
- (ii) the reason for the threefold coordination is a gallium vacancy on a neighbouring cation site.

The proposed structural model of the complex is shown in figure 8.

It should be mentioned that both recent theoretical as well as experimental findings favour the existence of nitrogen-related gallium vacancy defects [48, 49]. Density-functional calculations [48] find a binding energy of 0.43 eV for the nitrogen–gallium vacancy complex in its triply negative charge state ($N-V_{Ga}^{3-}$). Investigations of epitaxially grown GaAsN layers by

¹ In relation to the total nitrogen concentration detected spectroscopically, the substitutional nitrogen concentration amounts to >99% in implanted layers and to >90% in nitrogen-rich bulk samples.

positron annihilation spectroscopy [49] reveal gallium vacancy defects related to the nitrogen content.

7. Conclusions

It has been shown that FTIR absorption spectroscopy is an extremely valuable tool for investigating nitrogen in GaAs-based materials. Nitrogen-related defects give rise to LVM absorption bands, which can be detected at low sample temperatures with high sensitivity. Information of the microscopic defect structure is obtained by the influence of the host and/or impurity isotope mass on the LVM frequency. The selective implantation of nitrogen isotopes in combination with annealing (RTA) is of particular importance for the generation of specific defects. The 472 cm^{-1} LVM of the substitutional nitrogen species, N_{As} , allows the quantitative assessment of the incorporation of nitrogen on lattice sites in thin epitaxial GaAsN and InGaAsN layers. Further systematic work is necessary in the InGaAsN alloy system, to elucidate the local coordination of nitrogen and indium for different growth techniques and annealing procedures.

Acknowledgments

Part of this work has been supported by the Deutsche Forschungsgemeinschaft (DFG). The author would like to thank Y V Gomeniuk for performing FTIR measurements and for many fruitful discussions. The author is also indebted to G Ebbinghaus, A Ramakrishnan and H Riechert for providing MBE and MOCVD layers, and G Lenk and B Wiedemann for performing nitrogen implantations and SSMS measurements (BW).

References

- [1] Thompson F, Morrison S R and Newman R C 1972 *Radiation Damage and Defects in Semiconductor Reading (Inst. Phys. Conf. Ser. 16)* p 371
- [2] Newman R C, Thompson F, Hyliands M and Peast R F 1972 *Solid State Commun.* **10** 505
- [3] Theis W M, Bajaj K K, Litton C W and Spitzer W G 1982 *Appl. Phys. Lett.* **41** 70
- [4] Newman R C 1994 *Semicond. Sci. Technol.* **9** 1749
- [5] Pearton S J, Corbett J W and Stavola M 1992 *Hydrogen in Crystalline Semiconductors* (Berlin: Springer)
- [6] Schneider J, Dischler B, Seelewind H, Mooney P M, Lagowski J, Matsui M, Beard D R and Newman R C 1989 *Appl. Phys. Lett.* **54** 1442
- [7] Alt H Ch 1991 *Semicond. Sci. Technol.* **6** B121
- [8] Kachare A H, Spitzer W G, Kahan A, Euler F K and Whatley T A 1973 *J. Appl. Phys.* **44** 4393
- [9] Schwabe R, Seifert W, Bugge F, Bindemann R, Agekyan V F and Pogarev S V 1985 *Solid State Commun.* **55** 167
- [10] Riede V, Neumann H, Sobotta H, Schwabe R, Seifert W and Schwetlick S 1986 *Phys. Status Solidi a* **93** K151
- [11] Clerjaud B, Cote D, Hahn W S, Lebkiri A, Ulrici W and Wasik D 1997 *Phys. Status Solidi a* **159** 121
- [12] Weyers M, Sato M and Ando H 1992 *Japan. J. Appl. Phys.* **31** L853
- [13] Kondow M, Kitatani T, Nakatsuka S, Larson M C, Nakahara K, Yazawa Y, Okai M and Uomi K 1997 *IEEE J. Sel. Top. Quantum Electron.* **3** 719
- [14] Spruytte S G, Coldren C W, Harris J S, Wampler W, Krispin P, Ploog K and Larson M C 2001 *J. Appl. Phys.* **89** 4401
- [15] Grenouillet L, Bru-Chevallier C, Guillot G, Gilet P, Ballet P, Duvaut P, Rolland G and Million A 2002 *J. Appl. Phys.* **91** 5902
- [16] Wiedemann B, unpublished
- [17] Cochran W, Fray S J, Johnson F A, Quarrington J E and Williams N 1961 *J. Appl. Phys.* **32** 2102
- [18] Thomas D G and Hopfield J J 1966 *Phys. Rev.* **150** 680
- [19] Alt H Ch, Egorov A Yu, Riechert H, Wiedemann B, Meyer J D, Michelmann R W and Bethge K 2000 *Appl. Phys. Lett.* **77** 3331

- [20] Robbie D A, Leigh R S and Sangster M J L 1997 *Phys. Rev. B* **56** 1381
- [21] Leigh R S, Newman R C, Sangster M J L, Davidson B R, Ashwin M J and Robbie D A 1994 *Semicond. Sci. Technol.* **9** 1054
- [22] Alt H Ch, Wiedemann B and Bethge K 1997 *Materials Science Forum* vol 258–63 (Zurich: Trans Tech) p 867
- [23] Elliot R J, Hayes W, Jones G D, MacDonald H F and Sennett C T 1965 *Proc. R. Soc. A* **289** 1
- [24] Newman R C 1973 *Infra-Red Studies of Crystal Defects* (London: Taylor and Francis)
- [25] Ramakrishnan A, Ebbinghaus G and Stolz W 2002 *Inst. Phys. Conf. Ser.* **170** 825
- [26] Ahlgren T, Vainonen-Ahlgren E, Likonen J, Li W and Pessa M 2002 *Appl. Phys. Lett.* **80** 2314
- [27] Alt H Ch, Gomeniuk Y, Ebbinghaus G, Ramakrishnan A and Riechert R 2003 *Semicond. Sci. Technol.* **18** 303
- [28] Leigh R S and Newman R C 1988 *Semicond. Sci. Technol.* **3** 84
- [29] McKay H A, Feenstra R M, Schmidling T and Pohl U W 2001 *Appl. Phys. Lett.* **78** 82
- [30] Prokofyeva T, Saucy T, Seon M, Holtz M, Qiu Y, Nikishin S and Temkin H 1998 *Appl. Phys. Lett.* **73** 1409
- [31] Mascarenhas A and Seong M J 2002 *Semicond. Sci. Technol.* **17** 823
- [32] Kim K and Zunger A 2001 *Phys. Rev. Lett.* **86** 2609
- [33] Alt H Ch, Egorov A Yu, Riechert H, Meyer J D and Wiedemann B 2001 *Physica B* **308–10** 877
- [34] Sangster M J L, Newman R C, Geldhill G A and Upadhyay S B 1992 *Semicond. Sci. Technol.* **7** 1295
- [35] Kurtz S, Webb J, Gedvilas L, Friedman D, Geisz J, Olsen J, King R, Joslin D and Karam N 2001 *Appl. Phys. Lett.* **78** 748
- [36] Kitatani T, Kondow M and Kudo M 2001 *Japan. J. Appl. Phys.* **40** L750
- [37] Wagner J, Geppert T, Köhler K, Ganser P and Herres N 2001 *J. Appl. Phys.* **90** 5027
- [38] Lordi V, Gambin V, Friedrich S, Funk T, Takizawa T, Uno K and Harris J S 2003 *Phys. Rev. Lett.* **90** 145505
- [39] Ciatto G, D’Acapito F, Grenouillet L, Mariette H, De Salvador D, Bisognin G, Carboni R, Floreano L, Gotter R, Mobilio S and Boscherini F 2003 *Phys. Rev. B* **68** 161201
- [40] Gärtner G, Flade T, Jurisch M, Köhler A, Korb J, Kretzer U and Weinert B 1999 *J. Cryst. Growth* **198/199** 355
- [41] Theis W M, Bajaj K K, Litton C W and Spitzer W G 1982 *Appl. Phys. Lett.* **41** 70
- [42] Alt H Ch, Gomeniuk Y V and Wiedemann B 2004 *Phys. Rev. B* **69** 125214
- [43] Collins J D, Gledhill G A, Murray R, Nandra P S and Newman R C 1989 *Phys. Status Solidi b* **151** 469
- [44] Gledhill G A, Upadhyay S B, Sangster M J L and Newman R C 1991 *J. Mol. Struct.* **247** 313
- [45] Wilson E B, Decius J C and Cross P C 1980 *Molecular Vibrations* (New York: Dover)
- [46] Leigh R S and Newman R C 1988 *Semicond. Sci. Technol.* **3** 84
- [47] Kent P R C and Zunger A 2001 *Phys. Rev. B* **64** 115208
- [48] Janotti A, Zhang S B, Wei S H and Van de Walle C G 2003 *Phys. Rev. B* **67** 161201
- [49] Toionen J, Hakkarainen T, Sopanen M, Lipsanen H, Oila J and Saarinen K 2003 *Appl. Phys. Lett.* **82** 40